

A Hierarchical Variational Bayesian Approximation Approach in Acoustic Imaging

Ning Chu^{*,†}, Ali Mohammad-Djafari^{*}, Nicolas Gac^{*} and José Picheral^{**}

**Laboratoire des signaux et systèmes (L2S), CNRS-SUPELEC-UNIV PARIS-SUD, France*

†College of Electrical Science and Engineering, National University of Defense Technology, China

***Dept. Signal et Systèmes Électroniques, École Supérieure d'Électricité (SUPELEC), France*

Abstract. Acoustic imaging is a powerful technique for acoustic source localization and power reconstruction from limited noisy measurements at microphone sensors. But it inevitably confronts a very ill-posed inverse problem which causes unexpected solution uncertainty. Recently, the Bayesian inference methods using sparse priors have been effectively investigated. In this paper, we propose to use a hierarchical variational Bayesian approximation for robust acoustic imaging. And we explore the Student-t priors with heavy tails to enforce source sparsity, and to model non-Gaussian noise respectively. Compared to conventional methods, the proposed approach can achieve the higher spatial resolution and wider dynamic range of source powers for real data from automobile wind tunnel.

Keywords: Acoustic imaging; Variational Bayesian Approximation; Student-t prior; Non-Gaussian noise

PACS: 43.60.+d, 02.50.Cw, 07.05.Pj

INTRODUCTION

Nowadays, acoustic imaging methods play more and more important roles in industry for which we to take the (aero)acoustics performance into account, such as vehicle design, noise control and wind energy generation etc. In general, the conventional Beamforming method [1] can give a direct and fast acoustic power imaging, but its spatial resolution is often very coarse at low frequencies. Based on the beamforming, the forward model of acoustic power propagation can be modeled by a determined linear system of equations in frequency domain [2]: $\mathbf{y} = \mathbf{C}\mathbf{x}$, where $\mathbf{x} \in \mathbb{R}^{N \times 1}$ denotes the unknown acoustic power vector on the source plane consisted of N identical patches; $\mathbf{y} \in \mathbb{R}^{N \times 1}$ denotes the observed beamforming power vector at microphone array; $\mathbf{C} \in \mathbb{R}^{N \times N}$ denotes the source power propagation matrix, which not only depends on the geometric distance between the source and sensor, but also relies on the array geometry for a given frequency. The matrix \mathbf{C} is usually a shift-variant singular matrix, thus the problem of solving $\mathbf{y} = \mathbf{C}\mathbf{x}$ will be ill-posed. Recently, the Deconvolution Approach for Mapping of Acoustic Source (DAMAS) method [2] has been effectively applied in wind tunnel experiments by NASA. For super resolution imaging under strong Gaussian noise, many methods with sparsity constraints have been extensively developed [3]. However, the sparsity parameters have to be selected empirically. In order to obtain the robust parameter estimations, the Bayesian inference approaches with the sparsity favoring priors have been widely investigated [5, 6, 7, 8]. We propose to use the Double Exponential (DE) prior, and apply the joint Maximum A Posteriori (MAP) estimation [9] to improve upon

the DAMAS and its extensions. However, the joint MAP method often suffers from the time-consuming non-quadratic optimization.

In this paper, our motivation aims to obtain the robust acoustic imaging on the vehicle surface in wind tunnel tests, which will visualize the aeroacoustic performance of a car. To overcome the limitations of joint MAP, we propose to use the hierarchical Bayesian inference via Variational Bayesian Approximation (VBA). Moreover, Student-t priors are used to not only enforce the sparsity of source power distribution, but also to model the non-Gaussian distributed noise. This paper is organized as follows: we first introduce the forward model of acoustic power propagation. The proposed VBA approach is then discussed and used to solve the forward model. Subsequently, the method validation is carried out on simulations and real data respectively, and followed by our conclusions.

PROBLEM STATEMENT

We consider K unknown sources on the source plane and M number of microphone sensors located on a non-uniform 2D array. Before modeling, some assumptions are made: The acoustic sources are uncorrelated, monopoles [2]; Microphone sensors are omni-directional with unitary gain; In addition, complex reverberations in open wind tunnel are ignored.

After discretizing the source plane into N identical patches ($N \gg K$), we get N potential sources within which only K real sources are present non-zero items. So that it is beneficial to consider this as a sparse-vector of length N with K components. We should note that background noise in wind tunnel is mainly composed by the noise at the sensors, and the model uncertainty [9] caused by acoustic multi-path propagations such as reflection and refraction. In this case, the background noise should not be modeled by the ideal Gaussian white spectrum [2, 9], but by non-Gaussian colored noise. Therefore we propose the forward model of acoustic power propagation in colored noise as:

$$\mathbf{y} = \mathbf{C}\mathbf{x} + \xi, \quad (1)$$

where ξ denote the colored noise vector; the propagation matrix $\mathbf{C} = \{\|\mathbf{a}_i^H \mathbf{a}_j\|_2^2 / \|\mathbf{a}_i\|_2^2\}_{N \times N}$ is derived in [9], where the beamforming steering vector $\mathbf{a}_i = \left\{ \frac{\exp[-j2\pi f r_{i,m}]/c_0}{r_{i,m}} \right\}_{M \times 1}$ [2] depends on the geometric distance $r_{i,m}$ between source i and sensor m at a given frequency f , with c_0 being the acoustic speed in the air. Thus we can see that (1) is a determined system of linear equations in unknown \mathbf{x} , interference ξ and known \mathbf{y} .

PROPOSED VBA INFERENCE APPROACH

For the inverse problem in (1), some prior knowledge or necessary constraints on source powers \mathbf{x} and colored noise ξ should be investigated in order to reduce the solution uncertainty. Let \mathbf{y} denote the observed data, and θ the unknown parameters. The regularized inverse problem based on priors can be solved by the following Bayesian inference approaches [5, 6]: If we assign the specific prior probability $p(\xi)$ to noise vector ξ , we can define the likelihood $p(\mathbf{y}|\mathbf{x}, \theta)$, namely $p(\xi) = p(\mathbf{y} - \mathbf{x}|\theta)$,

which can be solved by the classical Maximum Likelihood (ML) estimation as $(\hat{\mathbf{x}}, \hat{\boldsymbol{\theta}})_{ML} = \arg \max_{\mathbf{x}, \boldsymbol{\theta}} \{p(\mathbf{y}|\mathbf{x}, \boldsymbol{\theta})\}$. In the Bayesian approach, we also assign specific prior probabilities $p(\boldsymbol{\xi}, \boldsymbol{\theta})$ to all unknown parameters. According to Baye's rule, we apply the joint MAP estimation to get:

$(\hat{\mathbf{x}}, \hat{\boldsymbol{\theta}})_{JMAP} = \arg \max_{\mathbf{x}, \boldsymbol{\theta}} \{ \ln p(\mathbf{x}, \boldsymbol{\theta}|\mathbf{y}) \} \propto \arg \min_{\mathbf{x}, \boldsymbol{\theta}} \{ -\ln p(\mathbf{y}|\mathbf{x}, \boldsymbol{\theta}) - \ln p(\mathbf{x}) - \ln p(\boldsymbol{\theta}) \}$. The joint MAP exploit the prior models of the unknowns to regularize the ML estimation. Compared to conventional regularization methods [3, 4], the joint MAP has the advantage of an adaptive estimation of the regularization parameter. However, $\ln p(\mathbf{x}, \boldsymbol{\theta}|\mathbf{y})$ cannot be obtained analytically for the present problem, and the joint MAP usually requires a nonlinear optimization. Moreover, both ML and joint MAP are the point estimators which can hardly consider the estimation precision.

The above difficulties of joint MAP can be overcome by the VBA [7, 8] inference. That is the posterior $p(\mathbf{x}, \boldsymbol{\theta}|\mathbf{y})$ can be approximated by a family of basic and easily-handled probability distributions $q(\mathbf{x}, \boldsymbol{\theta})$, satisfying $p(\mathbf{x}, \boldsymbol{\theta}|\mathbf{y}) \approx q(\mathbf{x}, \boldsymbol{\theta})$; and proper $q(\mathbf{x}, \boldsymbol{\theta})$ are estimated by maximizing variational bound $\mathcal{L}(\mathbf{x}, \boldsymbol{\theta})$ as: $\hat{q}(\mathbf{x}, \boldsymbol{\theta}) = \arg \max_{q(\mathbf{x}, \boldsymbol{\theta})} \{ \mathcal{L}(\mathbf{x}, \boldsymbol{\theta}) \}$, where $\mathcal{L}(\mathbf{x}, \boldsymbol{\theta}) = \int q(\mathbf{x}, \boldsymbol{\theta}) \ln \frac{p(\mathbf{y}, \mathbf{x}, \boldsymbol{\theta})}{q(\mathbf{x}, \boldsymbol{\theta})} d\boldsymbol{\theta} d\mathbf{x}$. Generally, $(\mathbf{x}, \boldsymbol{\theta})$ are supposed to be mutually independent as $q(\mathbf{x}, \boldsymbol{\theta}) = q_1(\mathbf{x}) \prod_i q_2(\boldsymbol{\theta}_i)$. Then $\mathcal{L}(\mathbf{x}, \boldsymbol{\theta})$ can be maximized by the mean field approximation [11] as $\hat{q}_2(\boldsymbol{\theta}_i) = \frac{\exp[I(\mathbf{x}, \boldsymbol{\theta}_i)]}{\int \exp[I(\mathbf{x}, \boldsymbol{\theta}_i)] d\boldsymbol{\theta}_i}$, where $I(\cdot)$ denotes the partition function, defined as $I(\mathbf{x}, \boldsymbol{\theta}_i) = \langle \ln p(\mathbf{y}, \mathbf{x}, \boldsymbol{\theta}) \rangle_{q_2(\boldsymbol{\theta}_{-i})} = \int q_2(\boldsymbol{\theta}_{-i}) \ln p(\mathbf{y}, \mathbf{x}, \boldsymbol{\theta}) d\boldsymbol{\theta}_{-i}$, where $\boldsymbol{\theta}_{-i}$ denote a parameter vector except the item $\boldsymbol{\theta}_i$. However, $I(\mathbf{x}, \boldsymbol{\theta}_i)$ can hardly be analytically computed, since it depends on $q_2(\boldsymbol{\theta}_{-i})$. But the approximating posterior $\hat{q}(\boldsymbol{\theta})$ can still be obtained owing to the conjugate priors [11]. For example, if $p(\boldsymbol{\theta})$ is assigned by a Gamma distribution and the likelihood $p(\mathbf{y}|\mathbf{x}, \boldsymbol{\theta})$ is modeled by the Gaussian, then $\hat{q}_2(\boldsymbol{\theta})$ will be another Gamma distribution, which belongs to the same family as $p(\boldsymbol{\theta})$.

Heavy tail prior for colored background noise

In wind tunnel experiments, we model the colored noise $\boldsymbol{\xi}$ by the Student-t prior distribution $St(\boldsymbol{\xi})$ which has a long heavy tail, rather than the Gaussian distortions whose thin tail excessively penalizes large errors of forward model. Another attractive superposition property is that $St(\boldsymbol{\xi})$ can be generated by marginalizing a hidden variable \mathbf{v} as $St(\boldsymbol{\xi}) = \int p(\boldsymbol{\xi}|\mathbf{v})p(\mathbf{v})d\mathbf{v}$, in which, the conditional prior $p(\boldsymbol{\xi}|\mathbf{v}) = \mathcal{N}(\boldsymbol{\xi}|0, \Sigma_{\boldsymbol{\xi}}^{-1})$ is the multivariate Gaussian distribution, with $\Sigma_{\boldsymbol{\xi}} = \text{Diag}\{\mathbf{v}\} \in \mathbb{R}^{N \times N}$ being noise covariance matrix; $\text{Diag}(\cdot)$ denote diagonal matrix; $\mathbf{v} = \{v_n\}_N \in \mathbb{R}^{N \times 1}$ denote the noise precision vector; and the hyper-prior $p(\mathbf{v})$ is the Gamma distribution: $p(\mathbf{v}) = \prod_{n=1}^N \mathcal{G}(v_n|a_v, b_v) = \prod_{n=1}^N \Gamma(a_v)^{-1} (b_v)^{a_v} v_n^{a_v-1} e^{-b_v v_n}$, with a_v, b_v being the hyper-parameters of $p(\mathbf{v})$, and $\Gamma(x) = \int t^{x-1} e^{-t} dt$.

According to proposed forward model of (1), the likelihood $p(\mathbf{y}|\mathbf{x}, \mathbf{v})$ is determined by the conditional prior $p(\boldsymbol{\xi}|\mathbf{v}) = \mathcal{N}(\boldsymbol{\xi}|0, \Sigma_{\boldsymbol{\xi}}^{-1})$ as:

$$p(\mathbf{y}|\mathbf{x}, \mathbf{v}) = \frac{|\Sigma_{\boldsymbol{\xi}}|^{1/2}}{(2\pi)^{N/2}} e^{-\frac{1}{2}(\mathbf{y}-\mathbf{C}\mathbf{x})^H \Sigma_{\boldsymbol{\xi}} (\mathbf{y}-\mathbf{C}\mathbf{x})}, \quad (2)$$

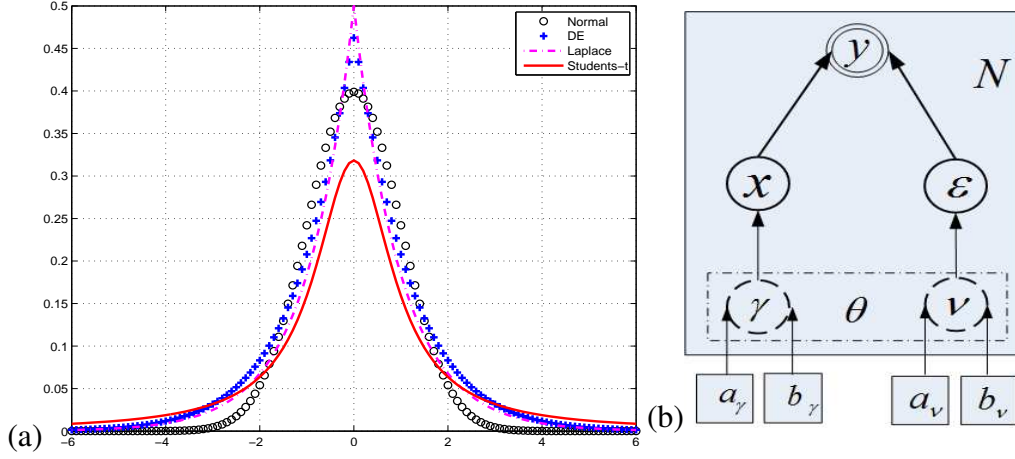


FIGURE 1. (a) Sparse priors on Gaussian normal, Laplace, DE and Student-t; (b) N dimension hierarchical Bayesian Graphical model; Double circle: observed data; Single: unknown variables; Dash: hidden variables; Square: hyper-parameters; Arrow: dependence.

where operator $(\cdot)^H$ denotes conjugate transpose.

Sparse prior on acoustic power image

Acoustic source in wind tunnel experiments are generated by the interaction of the air flow with special parts of the vehicle surface. Therefore, sources are located on some particular locations, while on the other parts, there is nearly no emission. This is why the acoustic power \mathbf{x} becomes a K -sparsity signal when the source plane is discretized into N patches. Such a sparse distribution can be represented by the distribution that has a high probability density around zero (sparsity) and a long heavy tail (dynamic range).

Here we apply the Student-t prior $St(\mathbf{x})$ [7] to enforce the sparsity and wide dynamic range of source power distribution. Owing to the superposition property of Student-t prior, the hidden variable γ is marginalized out for $St(\mathbf{x}) = \int p(\mathbf{x}|\gamma) p(\gamma) d\gamma$, where $p(\mathbf{x}|\gamma) = \mathcal{N}(\mathbf{x}|0, \Sigma_x^{-1})$ is assigned to multivariate Gaussian distribution, in which, Σ_x denote power covariance matrix, defined as $\Sigma_x = \text{Diag}\{\gamma\} \in \mathbb{R}^{N \times N}$ with $\gamma = \{\gamma_n\}_N \in \mathbb{R}^{N \times 1}$ being the power precision vector; and $p(\gamma) = \prod_{n=1}^N \mathcal{G}(\gamma_n|a_\gamma, b_\gamma)$, where a_γ, b_γ denote the hyper-parameters of $p(\gamma)$. $0 < \gamma_n < 1$ can greatly promote the sparsity as shown by the solid curve in Fig.1a; while for $\gamma_n \rightarrow \infty$, $St(x_n)$ approaches a Gaussian normal distribution as shown by the circle curve. Compared to the Double Exponential (DE) prior in the dot, $St(x_n)$ can have different γ_n for each x_n , while the DE prior requires precisely only two parameters for all \mathbf{x} in order to achieve the similar sparsity. In addition, the Laplacian distribution in dash curve belongs to the DE family.

VBA parameter estimations

In Fig. 1a, the graphical model [11] describes the dependencies between the observed data \mathbf{y} , all of the unknown variables \mathbf{x} , as well as the hidden variables $\theta = [\gamma, \mathbf{v}]^T$ and the initialized hyper-parameters $\phi_0 = [a_\gamma^0, b_\gamma^0, a_v^0, b_v^0]^T$. According to Bayes' rule, we have $p(\mathbf{x}, \theta | \mathbf{y}, \phi_0) \propto p(\mathbf{y} | \mathbf{x}, \theta, \phi_0) p(\mathbf{x} | \theta, \phi_0) p(\theta | \phi_0)$. Then by using the multivariate Gaussian likelihood in (2) and the superpositions of Student-t priors on \mathbf{x} and ξ , we can write the posterior as

$$p(\mathbf{x}, \theta | \mathbf{y}, \phi_0) = \mathcal{N}(\mathbf{x} | \mathbf{y} - \mathbf{C}\mathbf{x}, \Sigma_\xi^{-1}) \mathcal{N}(\mathbf{x} | 0, \Sigma_x^{-1}) \mathcal{G}(\gamma | a_\gamma^0, b_\gamma^0) \mathcal{N}(\xi | 0, \Sigma_\xi^{-1}) \mathcal{G}(\mathbf{v} | a_v, b_v^0) . \quad (3)$$

Due to the conjugate prior, the approximating posterior belongs to the Student-t distribution which is expressed by the multivariate Gaussian distribution $\hat{q}(\mathbf{x})$ and Gamma distribution $\hat{q}(\gamma)$, similarly for $\hat{q}(\mathbf{v})$ as follows:

$$\begin{cases} \hat{q}(\mathbf{x}) = \mathcal{N}(\mathbf{x} | \hat{\boldsymbol{\mu}}_x, \hat{\Sigma}_x) \\ \hat{q}(\gamma) = \prod_{n=1}^N \mathcal{G}(\gamma_n | \hat{a}_\gamma, \hat{b}_\gamma^n) \\ \hat{q}(\mathbf{v}) = \prod_{n=1}^N \mathcal{G}(\mathbf{v}_n | \hat{a}_v, \hat{b}_v^n), \end{cases} \quad (4)$$

where the averaged image $\hat{\boldsymbol{\mu}}_x$ is our final goal; the covariance matrix $\hat{\Sigma}_x$ offers the estimation precision by the VBA approach; and the expected variable estimates are:

$$\begin{cases} \hat{\boldsymbol{\mu}}_x = \hat{\Sigma}_x \mathbf{C}^T \langle \Sigma_\xi \rangle \mathbf{y} \\ \hat{\Sigma}_x = (\mathbf{C}^T \langle \Sigma_\xi \rangle \mathbf{C} + \langle \Sigma_x \rangle)^{-1} \\ \hat{a}_\gamma = a_\gamma^0 + \frac{N}{2}, \quad \hat{b}_\gamma^n = b_\gamma^0 + \frac{1}{2} \langle \mathbf{x}\mathbf{x}^T \rangle_{nn} \\ \hat{a}_v = a_v^0 + \frac{N}{2}, \quad \hat{b}_v^n = b_v^0 + \frac{1}{2} \langle \xi \xi^T \rangle_{nn} \end{cases} , \quad (5)$$

where the operator $(\cdot)_{nn}$ denotes the n th diagonal item, and $\langle \cdot \rangle$ denotes expectation, which is calculated as (see more details in [11, 7, 8].):

$$\begin{cases} \langle \Sigma_\xi \rangle = \text{Diag}\{\langle v_n \rangle\}_N = \text{Diag}\{\langle \hat{a}_v / \hat{b}_v^n \rangle\}_N \\ \langle \Sigma_x \rangle = \text{Diag}\{\langle \gamma_n \rangle\}_N = \text{Diag}\{\langle \hat{a}_\gamma / \hat{b}_\gamma^n \rangle\}_N \\ \langle \mathbf{x}\mathbf{x}^T \rangle = \hat{\boldsymbol{\mu}}_x \hat{\boldsymbol{\mu}}_x^T + \hat{\Sigma}_x \\ \langle \xi \xi^T \rangle = \mathbf{y}\mathbf{y}^T - 2\mathbf{C}\hat{\boldsymbol{\mu}}_x \mathbf{y}^T + \mathbf{C} \langle \mathbf{x}\mathbf{x}^T \rangle \mathbf{C}^T \end{cases} . \quad (6)$$

Computational analysis

From the solutions in (5), $\hat{\Sigma}_x$ involves the matrix inversion which cannot be calculated explicitly. We suggest to approximate $\hat{\Sigma}_x$ with a circulant matrix as $\hat{\Sigma}_x \approx (\langle \bar{v} \rangle \mathbf{C}^H \mathbf{C} + \langle \bar{\gamma} \rangle)^{-1}$, where $\bar{v} = \sum_{n=1}^N v_n$, $\bar{\gamma} = \sum_{n=1}^N \gamma_n$ denote the arithmetic means. Then the products of circulant matrices can be efficiently computed in the Discrete Fourier Transform (DFT) domain. In (5), the estimated expectation $\hat{\boldsymbol{\mu}}_x$ of the source powers can be analytically expressed as $\hat{\Sigma}_x^{-1} \hat{\boldsymbol{\mu}}_x = \mathbf{C}^H \langle \Sigma_\xi \rangle \mathbf{y}$. This linear system of equations is

solved iteratively with a conjugate gradient algorithm, which requires $O(N \log N)$ computations per iteration to solve for a solution vector \mathbf{x} of size N . If Q iterations are needed, total computations are of $O(QN \log N)$, which is computationally moderate.

SIMULATIONS

The simulation configuration is based on the wind tunnel experiments in Fig.3a: the distance between sensor and source plane is 4.50m; and there are $M=64$ sensors; The source plane is discretized into $5\text{cm} \times 5\text{cm}$ grids. In Fig.2a, source powers \mathbf{x} are generated by 4 monopoles and 5 extended sources with 14dB dynamic range, and the image size is of 27×17 pixels. The colored noise is generated by using the Gaussian white noise filtered by a low pass filter (cut-off frequency 3000Hz), and the averaged Signal-to-Noise Ratio (SNR) is set to 0dB.

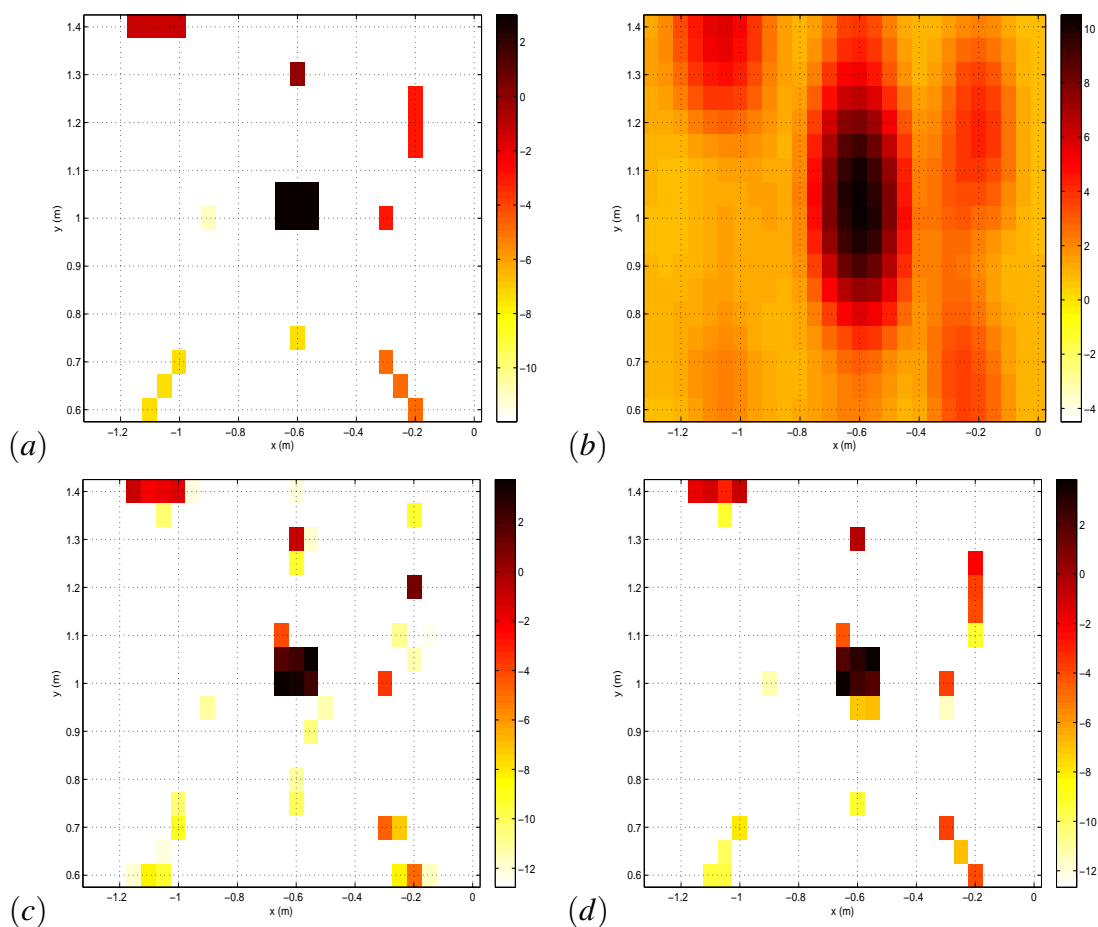


FIGURE 2. Simulation at 2500Hz, 0dB SNR under colored noise, 14dB span: (a) Source power distribution (b) Beamforming power (c) Bayesian joint MAP and (d) Proposed VBA inversion

In Fig.2b-d, the beamforming merely gives the strong sources and failed to distinguish most of the weak sources; our proposed VBA inference outperforms the joint MAP

method [9] due to its more precise localization and power estimation, especially for the better noise suppression.

WIND TUNNEL EXPERIMENTS

Wind tunnel experiments are designed to reconstruct the positions and acoustic powers on the traveling car surface. The grid is of 5cm , and source plane is thus of 31×101 pixels. The wind speed is 160km/h ; there are 524288 samples with the sampling frequency $f_s = 2.56 \times 10^4$ Hz. The total samples are organized into $I=204$ blocks with 2560 samples in each bloc. The working frequency is 2500Hz which is within the frequency range of the human acoustic perception. The image results are obtained in frequency domain shown by normalized dB images with 10dB span. The propagation matrix \mathbf{C} in (1) is rectified for the wind refraction and ground reflection as discussed in [9].

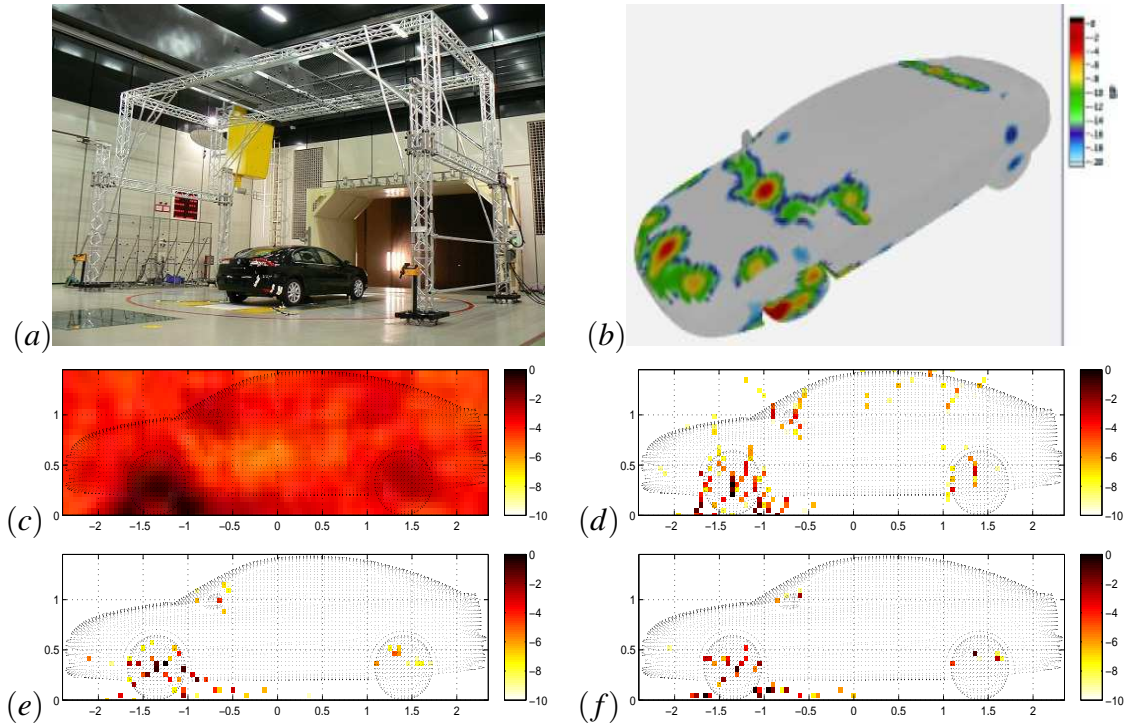


FIGURE 3. Vehicle acoustic imaging at 2500Hz: (a) Wind tunnel S2A Renault France [12](b) Acoustic imaging [12] (c) Beamforming (d) DAMAS (e) joint MAP and (f) Proposed VBA.

Fig.3a illustrates the Wind Tunnel S2A configuration, and Fig.3b give the result offered by Renault company researchers. Moreover, Fig.3c–f as well as the estimated powers of mentioned methods. Due to the high side-lobe effect, beamforming merely gives a fuzzy image of strong sources in Fig.3c; DAMAS successfully deconvolves the beamforming image and discovers sources around the wheels and rear-view mirror, however, many false targets are also detected on the air in Fig.3d; In Fig.3e and f, the joint MAP inference via DE prior [9] and proposed VBA inference not only manages to distinguish the strong sources around both wheels and rear-view mirror, but also successfully reconstructs the weak ones on the front cover and light. Furthermore,

the background noise suppression in proposed VBA is superior than others owing to Student-t prior.

CONCLUSION

We proposed a VBA inference via Student-t priors on the source power and colored noise for super spatial resolution, wide dynamic range and robust parameter estimation. On simulations and real data in wind tunnel, the proposed VBA approach has been validated by comparison to classical methods. However, the VBA still requires a huge amount of computation in calculating $\hat{\Sigma}_x \approx (\langle \bar{\mathbf{v}} \rangle \mathbf{C}^H \mathbf{C} + \langle \bar{\boldsymbol{\gamma}} \rangle)^{-1}$. For real-time processing, it needs to employ the Graphical Processing Unit (GPU) for hardware accelerations.

ACKNOWLEDGMENTS

We greatly thank Renault SAS for offering real data, and appreciate valuable comments from Prof. Udo von Toussaint of Max-Planck-Institut Germany, Dr. Frédérique Barbaresco of Thales France, as well as Prof. HUANG Xiaotao of NUDT University China.

REFERENCES

1. J. Chen, K. Yao, and R. Hudson, Source localization and beamforming, *Signal Processing Magazine, IEEE* **19**, 30–39 (2002).
2. T. Brooks, and W. Humphreys, A Deconvolution Approach for the Mapping of Acoustic Sources (DAMAS) determined from phased microphone arrays, *Journal of Sound and Vibration* **294**, 856–879 (2006), ISSN 0022-460X.
3. T. Yardibi, J. Li, P. Stoica, N. S. Zawodny, and L. N. Cattafesta, A covariance fitting approach for correlated acoustic source mapping, *Journal of The Acoustical Society of America* **127**, 2920–31 (2010).
4. N. Chu, J. Picheral, A. Mohammad-Djafari, and N. Gac, A robust super-resolution approach with sparsity constraint in acoustic imaging, *Applied Acoustics* **76**, 197–208 (2014).
5. G. Oliveri, P. Rocca, and A. Massa, A Bayesian-Compressive-Sampling-Based Inversion for Imaging Sparse Scatterers, *Geoscience and Remote Sensing, IEEE Transactions on* **49**, 3993–4006 (2011).
6. J. Antoni, A Bayesian approach to sound source reconstruction: optimal basis, regularization, and focusing, *The Journal of the Acoustical Society of America* **131**, 2873–2890 (2012).
7. D. Tzikas, A. Likas, and N. Galatsanos, Variational Bayesian sparse kernel-based blind image deconvolution with Student's-t priors, *IEEE Transactions on Image Processing* **18**, 753–764 (2009).
8. A. Mohammad-Djafari, Bayesian approach with prior models which enforce sparsity in signal and image processing, *EURASIP Journal on Advances in Signal Processing* **2012**, 52 (2012), ISSN 1687-6180.
9. N. Chu, A. Mohammad-Djafari, and J. Picheral, Robust Bayesian super-resolution approach via sparsity enforcing a priori for near-field aeroacoustic source imaging, *Journal of Sound and Vibration* **332**, 4369–4389 (2013), ISSN 0022-460X.
10. A. Massa, and G. Oliveri, Bayesian compressive sampling for pattern synthesis with maximally sparse non-uniform linear arrays, *IEEE Transactions on Antennas and Propagation* **59**, 467–681 (2011).
11. M. Jordan, Z. Ghahramani, T. Jaakkola, and L. Saul, An introduction to variational methods for graphical models, *Machine learning* **37**, 183–233 (1999).
12. A. Menoret, N. Gorilliot, and J.-L. Adam, Acoustic imaging in wind tunnel S2A, “Acoustic imaging in wind tunnel S2A,” in *10th Acoustics conference (ACOUSTICS2010)*, Lyon, France, 2010.